Heliyon 10 (2024) e40807

Contents lists available at ScienceDirect

Heliyon

journal homepage: www.cell.com/heliyon

Research article

Tactile imagery affects cortical responses to vibrotactile stimulation of the fingertip

Marina Morozova [a,*,1], Lev Yakovlev [a,b,**,1], Nikolay Syrov [a], Mikhail Lebedev [c,d], Alexander Kaplan [a,e]

[a] Vladimir Zelman Center for Neurobiology and Brain Rehabilitation, Skolkovo Institute of Science and Technology, 121205, Moscow, Russia
[b] Faculty of Biology, Shenzhen MSU-BIT University, 518115, Shenzhen, China
[c] Faculty of Mechanics and Mathematics, Lomonosov Moscow State University, 119991, Moscow, Russia
[d] Sechenov Institute of Evolutionary Physiology and Biochemistry of the Russian Academy of Sciences, 194223, Saint Petersburg, Russia
[e] Department of Human and Animal Physiology, Faculty of Biology, Lomonosov Moscow State University, 119234, Moscow, Russia

ARTICLE INFO

Keywords:
Tactile imagery
Somatosensory evoked potentials
Event-related desynchronization/ synchronization
EEG
Vibrotactile stimulation
Cerebral cortex
Working memory

ABSTRACT

Mental imagery is a crucial cognitive process, yet its underlying neural mechanisms remain less understood compared to perception. Furthermore, within the realm of mental imagery, the somatosensory domain is particularly underexplored compared to other sensory modalities. This study aims to investigate the influence of tactile imagery (TI) on cortical somatosensory processing. We explored the cortical manifestations of TI by recording EEG activity in healthy human subjects. We investigated event-related somatosensory oscillatory dynamics during TI compared to actual tactile stimulation, as well as somatosensory evoked potentials (SEPs) in response to short vibrational stimuli, examining their amplitude-temporal characteristics and spatial distribution across the scalp. EEG activity exhibited significant changes during TI compared to the no-imagery baseline. TI caused event-related desynchronization (ERD) of the contralateral μ-rhythm, with a notable correlation between ERD during imagery and real stimulation across subjects. TI also modulated several SEP components in sensorimotor and frontal areas, showing increases in the contralateral P100 and P300, contra- and ipsilateral P300, frontal P200, and parietal P600 components. The results clearly indicate that TI affects cortical processing of somatosensory stimuli, impacting EEG responses in various cortical areas. The assessment of SEPs in EEG could serve as a versatile marker of tactile imagery in practical applications. We propose incorporating TI in imagery-based brain-computer interfaces (BCIs) to enhance sensorimotor restoration and sensory substitution. This approach underscores the importance of somatosensory mental imagery in cognitive neuroscience and its potential applications in neurorehabilitation and assistive technologies.

* Corresponding author. Vladimir Zelman Center for Neurobiology and Brain Rehabilitation, Skolkovo Institute of Science and Technology, 121205, Moscow, Russia.
** Corresponding author. Vladimir Zelman Center for Neurobiology and Brain Rehabilitation, Skolkovo Institute of Science and Technology, 121205, Moscow, Russia.
E-mail addresses: M.Morozova@skoltech.ru (M. Morozova), leojackovlev@gmail.com (L. Yakovlev).
[1] joint first authorship, MM and LY both contributed equally to this work.

https://doi.org/10.1016/j.heliyon.2024.e40807
Received 14 June 2024; Received in revised form 22 November 2024; Accepted 27 November 2024
Available online 28 November 2024

1. Introduction

Human ability to imagine events, actions and perceptions [1,2] is of great interest to basic neuroscience [3–6] and practical applications in the clinic [7–11]. In the sensory domain, humans can imagine visual objects [12], sounds [13,14], smells [15,16], and tactile sensations [17,18]. Such sensory imagery engages mostly the same neural structures that are activated by the physical sensory inputs [19]. The research on sensory imagery has primarily focused on the visual modality [20,21]. In the sensorimotor domain, many studies have scrutinized motor imagery (MI) [9,22,23] but relatively few have examined imagined somatic sensations [17,18,24–26].

Here we conducted an electroencephalographic (EEG) study of tactile imagery (TI). In addition to the scientific inquiry, this work was motivated by a practical idea of adding TI to the design of brain-computer interfaces (BCIs) [18,25,27] where MI has been abundantly implemented and studied (*for review see* Ref. [28]). While MI-based BCIs engage brain areas that generate motor commands, TI-based BCIs could selectively engage the areas involved in somatosensory processing [17,24,29–31], which could be useful for rehabilitation of somatosensory disabilities. As such, TI-based BCIs have distinct clinical goals. While the effects of MI have been extensively studied in sensorimotor cortical networks with a range of methods, the effects of TI remain to be clarified, which would facilitate their incorporation in BCI applications.

In this study of TI, we examined EEG patterns. EEG data have been previously examined in the studies on motor control and MI with two major effects reported: event-related desynchronization/synchronization (ERD/S) and somatosensory evoked potentials. Thus, ERD/S of the EEG sensorimotor rhythms (SMR) (μ and β) has been observed during motor preparation, execution, imagery [32,33], and motor learning [34,35]. Generally, ERD of the μ rhythm is an indicator of increased processing of sensorimotor information [36, 37]. Moreover, in our previous study, we observed ERD during TI and tactile stimulation (TS) [18].

The experimental paradigm utilized in the present studyallowed for the measurement of somatosensory evoked potentials (SEPs) during TI. Different components of SEPs have been described in the previous literature. Thus, the early components of SEPs with the latency below 150 ms represent an activation of the primary somatosensory cortex (S1) [38]. The longer-latency SEP components contain the contribution of the other areas, such as the secondary somatosensory area (S2) [39]. We aimed to investigate the contribution of S1 and S2 during TI, as there is strong evidence for their involvement in tactile perception, integration, and somatic learning. Barsalou [40] and Schmidt et al. [24] suggested that S1 provides perceptual grounding during TI, and Yoo et al. [17] reported

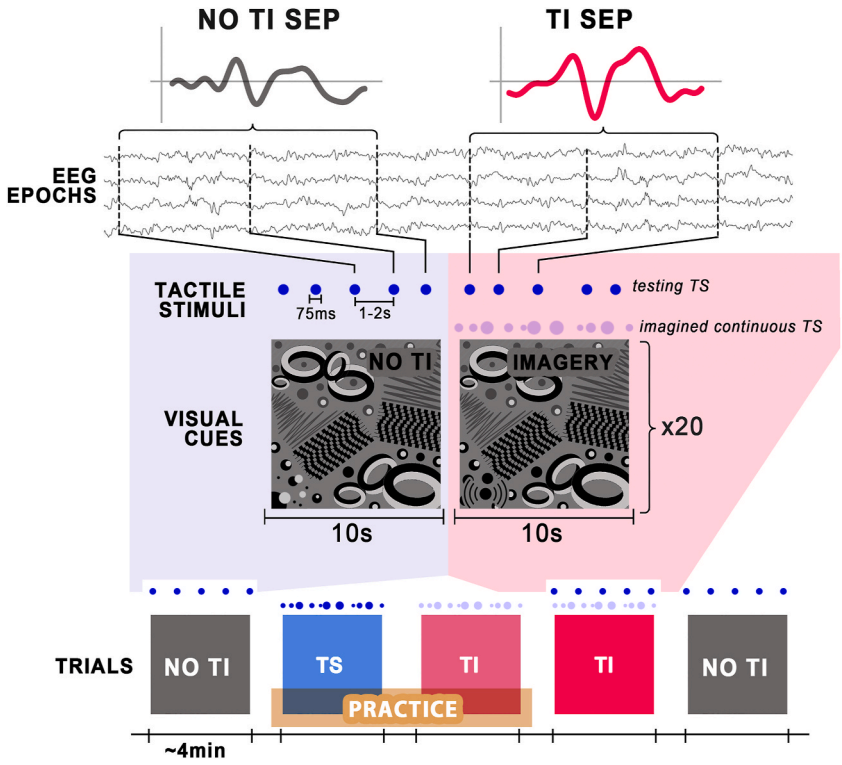

Fig. 1. The experimental sequence. The session started with a no-TI baseline condition (~4 min). Next, two practice conditions were run: the TS-practice where the participants got familiar with vibrostimulation in the form of randomized trials of vibratory stimuli applied to the right index fingertip, and the TI-practice where they mentally reproduced those sensations from vibrostimulation. The main experimental block followed then, which consisted of the TI condition. The heavy-blue dots represent vibrostimulation trains, and the light-blue dots represent the imagery of these trains. A no-TI baseline condition concluded the session. Somatosensory evoked potentials (SEPs) were induced by short (75 ms) vibratory pulses. These pulses are marked by small blue dots. Abbreviations: tactile stimulation (TS); tactile imagery (TI); somatosensory evoked potentials (SEP). (For interpretation of the references to colour in this figure legend, the reader is referred to the Web version of this article.)

that both S1 and S2 areas are activated during TI and TS. Based on this previous work, we hypothesized that both early and late SEP components would change during TI.

Our study adds to the previous work where functions of sensorimotor network were probed with different types of brief stimuli such as the study of Takemi et al. [41], Aono et al. [42], Vasilyev et al. [43] where TMS-evoked motor potentials were evaluated in the participants performing MI, and the study of [44,45] where the effects of MI on the spinal reflexes was examined. We focused on using a compatible approach in the somatosensory domain. We explored how TI modulated sensorimotor cortical processing by examining the changes in the amplitude and latency of the cortical responses to brief vibrotactile stimulation of the skin. We hypothesized that TI would modulate the amplitude of short-latency SEPs, with a predominant effect in the hemisphere contralateral to the imagined limb. We also expected to observe modulations of the longer-latency SEPs where TI could contribute a memory-based replay of the previous sensory experience.

2. Materials and methods

2.1. Subjects

Twenty nine healthy volunteers (9 females, 25.1 ± 4.8 y.o., right-handed) participated in one experimental session lasting up to 90 min.

2.2. Ethics and consent

The study was designed and conducted in accordance with the Declaration of Helsinki and the guidelines of the local ethics committee (the Institutional Review Board of the Skolkovo Institute of Science and Technology; protocol №10, May 18, 2023). All participants provided written informed consent before participating in the study.

2.3. Experimental design

The experimental session started with several practice runs, where subjects were trained on TI, followed by the experimental block where SEPs were measured in the absence of TI (*i.e.* no-TI baseline) and during TI (Fig. 1).

During the practice runs, the participants got familiar with continuous vibrostimulation applied to the right index fingertip and trained in mentally reproducing these tactile sensations. The practice runs consisted of two conditions: TS-practice where the subjects experienced vibrotactile stimulation and TI-practice where they imagined receiving vibrostimulation. During the TS-practice, the participants were instructed to memorize the skin sensations associated with the different characteristics of the stimulation, including skin pressure, tickling sensations, and intensity and duration of the stimuli. The TI-practice had two consecutive runs, each requiring tactile imagery in the absence of physical stimulation, which ensured that the participants learned this type of imagery. During these runs, the participants were instructed to recall their sensations experienced during the actual stimulation of the fingertip. While mentally reproducing these sensations, the subjects did not adhere to an imagery of a specific vibrotactile pattern. Instead, they were instructed to imagine randomly occurring bursts of vibration that had variable amplitude and duration. The practice runs consisted of a fixed number of trials. The TS-practice condition consisted of a total of 15 trials of vibrostimulation intermixed with 15 trials without stimulation (referred to as reference state). Stimulation trials consisted of 8-s trains of randomly patterned vibrations. The stimulus randomization reduced tactile habituation and helped to avoid residual tactile sensations. The reference state trials were the trials of the visual attention task where abstract graphical content was used such as dots, lines, loops, and helices with multiple intersections (Fig. 1). The participants were instructed to silently count the elements on the screen at a comfortable pace. This task had several purposes, including the cessation of mental imagery and prevention of mind wandering. The task also assured stable conditions where sensorimotor and visual processing were effectively separated, with a decrease in the occipital α-rhythms and an increase in the μ-rhythm [43,46]. The TI-practice trials were arranged similarly to the TS-practice trials, with the difference that vibrotactile stimulation was not used. The total number of the TI-practice trials was $n = 30$ (performed in two consecutive runs).

The main experimental block consisted of the no-TI condition that served as a baseline and the TI condition. SEPs were recorded for both conditions. To evoke SEPs, short (75 ms) testing vibrotactile pulses were applied to the right index fingertip, with the inter-stimulus interval varying from 1 to 2 s. During the no-TI baseline condition, vibrotactile pulses were applied whereas the participants were asked to direct their gaze to an abstract picture on the screen in front of them. The baseline runs were performed at the beginning and at the end of the experimental session. For the baseline runs, the number of vibrotactile pulses was $n = 200$ (100 per run). In the TI condition, participants were presented with an abstract image with a visual cue that required participants to perform tactile imagery for a period of 10 s, during which the abstract image was displayed on the screen. The abstract image served to control participants' visual attention by ensuring that their gaze remained fixed on the screen throughout the trial. The TI condition consisted of a total of 100 vibrotactile stimuli across all trials.

2.4. EEG data acquisition and analysis

Throughout the experiment, EEG data were collected using an NVX-52 amplifier (MCS, Russia). Forty seven EEG channels were recorded according to the international 10/10 montage with the sampling frequency of 500 Hz using *Ag/AgCl* electrodes lubricated by an electrode gel. The ground lead was attached to the *FCz* site. Two reference electrodes were placed on the left and right mastoids in

the positions of *TP9* and *TP10* channels. The skin-electrode impedance was kept below 15 kΩ. During the experimental session, participants were asked to keep their eyes open, sit still in a comfortable position and avoid movements while EEG recording was in progress. Visual stimuli were presented on the monitor placed at the distance of 1.2 m in front of the participant. The participants were asked to count random elements of the visual stimuli when they were present on the screen. Vibrostimulation was applied to the index fingertip of the right hand.

For EEG preprocessing, noisy channels were detected based on the signal-to-noise ratio for each participant and interpolated using spherical spline interpolation. The channel was considered noisy if its z-score deviated significantly from the median value or based on the signal-to-noise ratio if it had an abnormally high amount of high-frequency noise that was not correlated with the signals on any other channels [47]. The number of interpolated channels varied for each participant and did not exceed 11 %. The highest number of interpolated channels was n = 5 for one of the subjects, and the average number of interpolated channels was 1.93 ± 1.11 (mean ± standard deviation). Eye-movement artifacts were removed with an Independent Component Analysis (ICA) using *Fp1-Fp2* channels as EOG. The preprocessed EEG signals were band-pass filtered using a 4th order Butterworth filter in two frequency ranges: a) 0.2–12 Hz for ERP analysis in time domain, and b) 0.2–40 Hz for time-frequency analysis using the continuous Morlet wavelet transform (CWT).

To explore the dynamics of EEG oscillatory power in the TS and TI trials, CWT (*time window = 0.5 s; f0* = 3 Hz *central frequency; FWHM = 0.187 s*) was applied to each 8-s epoch of the practice runs. The resulting time-frequency matrices with CWT power were converted to ERD/S values using equation (11):

$$ERD = \frac{PSD_{smr} - PSD_{rst}}{PSD_{rst}}\ 100\% \tag{11}$$

where PSD_{smr} is the across-epoch average of CWT power for the TS or TI trials for each channel, and PSD_{rst} is the average CWT power calculated for the reference state epochs. Average ERD values over the trial duration (0–8 s) and individual μ-/β-ranges were used for topographic mapping.

For the SEPs analysis, EEG data were split into 1.5-s epochs starting 0.5 s before and ending 1 s after the vibratory pulse onset. Each epoch was z-score standardized. We calculated the amplitudes of P100, P200, P300 and P600 for each participant and each condition as the maximum values for the temporal-spatial range predefined by the cluster-based permutation test [48]. To analyze the time-frequency changes caused by the vibrotactile pulses, the CWT was applied to the 1.5-s epochs and ERD/S was calculated using equation (1). PSD_{rst} was calculated for the 0.5-s epochs preceding the visual cue. In the resulting time-frequency maps, latency and localization of spectral peaks and their median power were calculated for the temporal-spatial-frequency range predefined by cluster-based permutation test. We defined the individual frequencies of the μ- and β-rhythms for each participant based on the visual inspection of the spectra. The power of the μ- and β-rhythms was then more precisely calculated as the median value in the ±1 Hz window for the 8-s and 1.5-s wavelets.

2.5. Statistical analysis

In order to define the time intervals and channels with distinct SEP components, we compared the no-TI and TI SEPs using a cluster-based permutation test against zero. The cluster-based permutation test against zero was also used to define the time-frequency ranges where ERD/S was significantly different from zero. Because permutation tests tend to merge different physiological components into one statistically significant cluster and generate a wide range of statistically significant channel locations [49], we did not use the exact spatiotemporal and frequency ranges provided by the permutation tests but selected the ones that had a physiological explanation according to the literature. The effects of TI on the SEPs were then revealed using a pairwise comparison of the selected spatiotemporal features, and for the correlation analysis of the ERD/S was based on the selected spatiotemporal features in a specific frequency range. For pairwise comparison of the peak component amplitudes and median rhythm powers, Wilcoxon signed rank test was used (N = 29). Spearman's rank correlation coefficient was used to assess the relationship between the peak component amplitude and rhythm power. Nonparametric versions of pairwise test and correlation metric were chosen since in the case of relatively small sample size normality assumption was questionable.

2.6. Code/software

Visual stimuli were delivered using PsychoPy 2022.2.5. The post hoc preprocessing and analysis was performed using Python data processing packages, including MNE 1.3.1 and SciPy 1.10.0.

We used a custom designed and computer-controlled vibrotactile stimulator controlled by an Arduino UNO (Arduino, Italy). A flat vibration motor (6 mm in diameter, max speed of 12 000 rpm) was placed on the index finger of the right hand. In the 8-s trains of vibration, the motor speed was randomly patterned in the range 6 000–12 000 rpm. This random stimulation pattern reduced tactile habituation and minimized the residual tactile sensations following the vibration offset. During the short (75 ms) vibratory pulses, the motor speed was set at 9 000 rpm.

3. Results

3.1. Event-related desynchronization (ERD) during tactile imagery practice

During the 8-s practice trials of TS, we observed pronounced ERDs of the μ- and β-rhythm for the *C3* and *CP3* EEG channels (Fig. 2A and C). These ERDs were the strongest in the hemisphere contralateral to the site of vibrostimulation. The ipsilateral-hemisphere ERDs were noticeable for the *C4* and *CP4* channels, but these ERDs were still lower compared to the ERDs in the contralateral hemisphere ($W = 107$; $p = 0.0157$; N = 29).

The μ- and β-rhythm ERDs also occurred during the TI-practice. These ERDs had the same localization but lower intensity compared to the TS-practice ($W = 88$; $p = 0.0041$; N = 29). The tendency for the μ-rhythm ERDs to be stronger in the contralateral hemisphere was still present but lost statistical significance ($W = 164$; $p = 0.265$; N = 29).

For the μ-rhythm, the TS-practice ERDs and the TI-practice ERDs were strongly positively correlated in the across-participant analysis (Spearman's rank correlation, $r_S = 0.731$; $p < 0.0001$; N = 29), that is the participants that had a weak ERD during the TS-practice also had a weak ERD during the TI-practice and the participants with strong ERDs during the TS-practice had strong ERDs during the TI-practice (Fig. 3A). We also observed a correlation between the μ-rhythm spectral peak power in the reference state and the μ-rhythm ERD value during the TI-practice trials (Fig. 3B, Spearman's rank correlation, $r_S = -0.653$; $p = 0.0001$; N = 29). Note that 6 participants out of 29 were unable to voluntarily generate detectable μ-rhythm ERD. Additionally, note the difference in the individual μ-rhythm frequencies across the participants (Fig. 2D).

3.2. Somatosensory-evoked potentials (SEPs) in response to short vibratory pulses

The SEPs in response to 75-ms vibratory pulses consisted of four prominent components: a P100 response in the contralateral centro-parietal region (latency of ~103 ms; *CP3*, *P1*, *P3*, *P5* channels), a P200 response in the centro-frontal region (latency of ~227 ms; *F3*, *FC1*, *FC3*, *FCz*, *F4*, *FC2*, *FC4* channels), a P300 response in the contra- and ipsilateral central regions (latencies of ~302 and ~320 ms for the contra- and ipsilateral hemispheres, respectively; *C5*, *CP5* and *C6*, *CP6* channels), and a P600 response in the parietal region (latency of ~606 ms; *P1*, *Pz*, *P2*, *PO3*, *POz*, *PO4*). At the no-TI baseline condition, the P100 components were also noticeable in the corresponding regions of the ipsilateral hemisphere (latency of ~126 ms; *CP4*, *P2*, *P4*, *P6* channels, Fig. 4).

3.3. Time-frequency responses to short tactile stimuli

In the time-frequency maps for the responses to 75-ms vibratory pulses, we observed changes in the following time-frequency ranges: ERS of the θ-rhythm in the contralateral centro-parietal region (3–8 Hz, 100–300 ms; *Fz*, *F3*, *FCz*, *FC1*, *FC3* channels), and ERD of the μ- and β-rhythms (100–600 and 100–300 ms, correspondingly; *C1*, *C3*, *C5*, *CP1*, *CP3*, *CP5* channels) in the contra- and ipsilateral central regions (Figs. 5 and 7A).

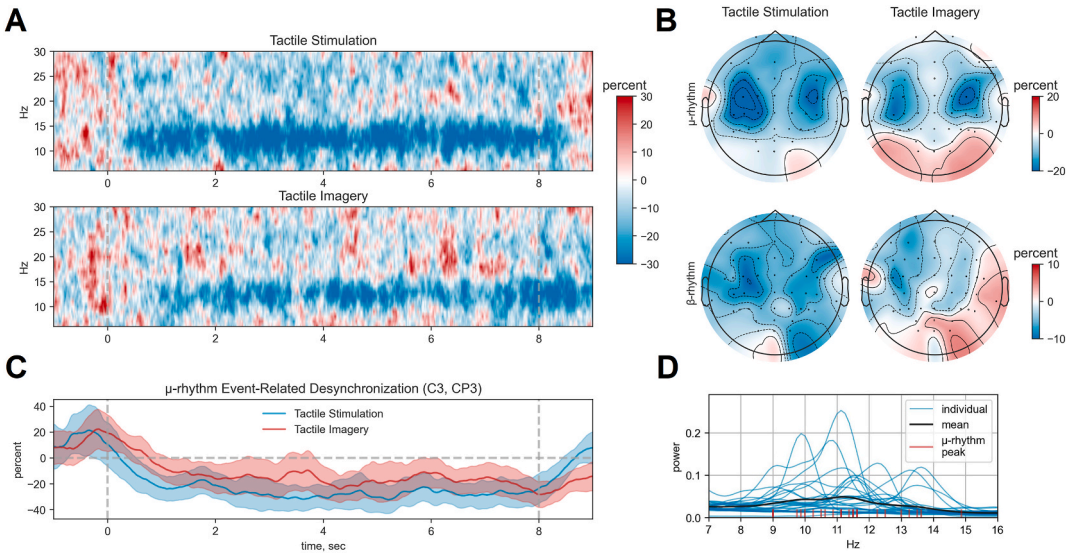

Fig. 2. Group changes (N = 29) in EEG activity during the practice runs. The TS-practice and TI-practice trials are shown separately. **A.** Time-frequency dynamics (percent change relative to the reference state) of the EEG spectral power during TS (top) and TI (bottom). **B.** Topographic maps of the μ- and β-rhythm ERD during TS and TI. **C.** Changes in time of the μ-rhythm ERD during TS and TI. **D.** Reference state spectra for the *C3* and *CP3* channels with marks showing individual μ-rhythm frequencies.

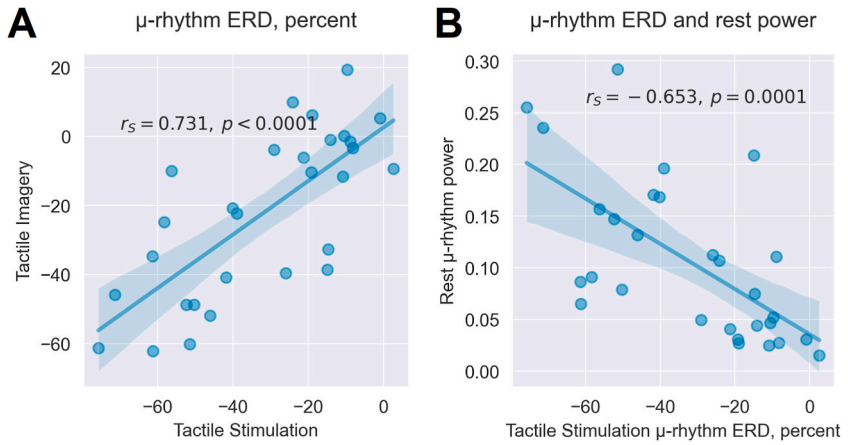

Fig. 3. The results of the correlational analysis for (A) the μ-rhythm ERD during TS versus TI and (B) the μ-rhythm ERD versus its power at the reference state.

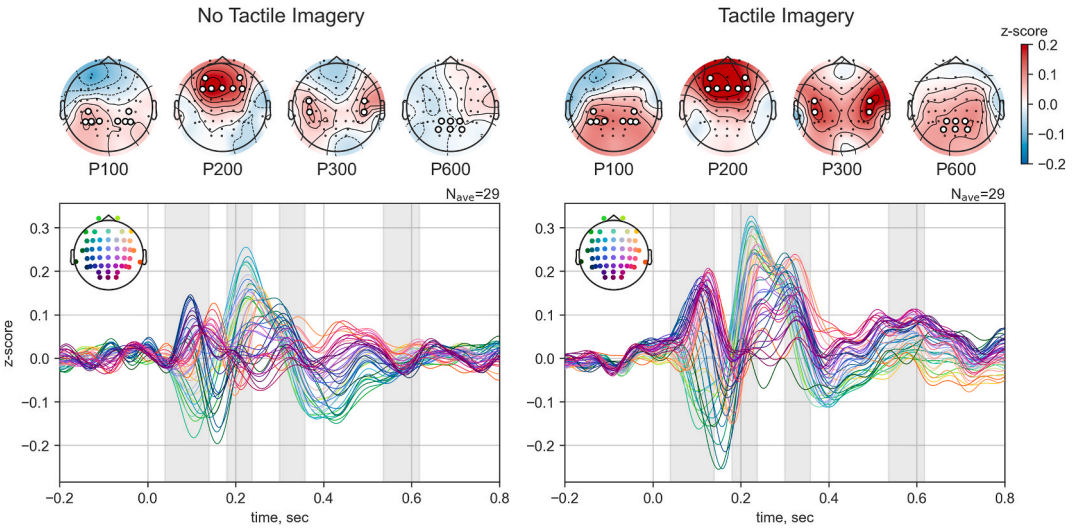

Fig. 4. Somatosensory Evoked Potentials (SEPs) in response to short (75 ms) vibrotactile pulses and localization of their components (P100, P200, P300, P600) for no-TI baseline condition and TI trials. The grand average across subjects (N = 29) is shown. The target channels for which the amplitudes of the components in the contra- and ipsi-lateral hemispheres were calculated are marked with white dots.

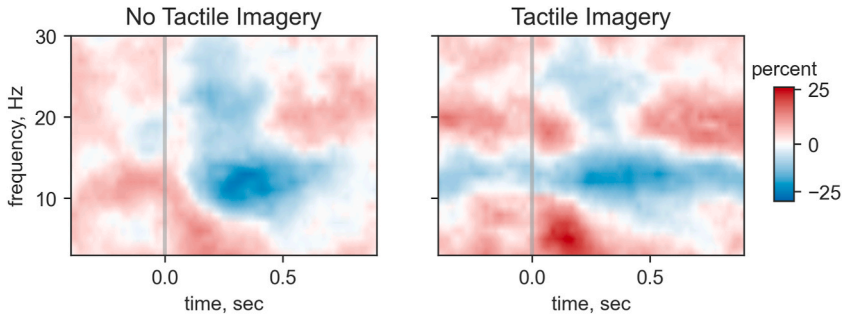

Fig. 5. Time-frequency maps of responses to 75-ms vibration pulses in the no-TI baseline condition and during continuous TI performance. The plots represent the average for the *C3* and *CP3* channels across participants.

3.4. Tactile imagery modulates ERPs and time-frequency responses

We did not find any statistically significant difference between the ERP peak amplitudes at the beginning and at the end of the experimental session ($W_{P100\_contra} = 111$; $p_{P100\_contra} = 0.265$; $W_{P100\_ipsi} = 98$; $p_{P100\_ipsi} = 0.137$; $W_{P200} = 107$; $p_{P200} = 0.219$; $W_{P300\_contra} = 96$; $p_{P300\_contra} = 0.122$; $W_{P300\_ipsi} = 139$; $p_{P300\_ipsi} = 0.753$; $W_{P600} = 129$; $p_{P600} = 0.549$; N = 29). Given that there was no difference between these conditions, we combined the last 50 epochs from the no-TI baseline conditions before and after the TI session (100 epochs in total) to obtain an average ERP in the absence of TI.

We compared the amplitudes of the contra- and ipsilateral P100, frontal P200, contra- and ipsilateral P300 and parietal P600 peaks during TI to the corresponding peaks in the average ERP in no-TI baseline and applied Holm-Sidak correction for multiple tests (Fig. 6A and B and 7).

We did not find statistically significant changes in the P100 peak amplitude during TI compared to average ERP in no-TI baseline in the contralateral hemisphere ($W = 127$; $p = 0.0506$; $p_{corr} = 0.0506$; N = 29) whereas there was statistically significant increase in P100 peak amplitude in the ipsilateral hemisphere ($W = 93$; $p = 0.006$; $p_{corr} = 0.0306$; N = 29).

We also found a statistically significant increase in the frontal P200 peak amplitude during TI compared to the average ERP in no-TI baseline ($W = 110$; $p = 0.019$; $p_{corr} = 0.0377$; N = 29).

There was a statistically significant increase in the P300 peak amplitude in both hemispheres and the P600 amplitude during TI compared to the average ERP in no-TI baseline (P300: $W_{contra} = 95$; $p_{contra} = 0.0069$; $p_{corr,\ contra} = 0.0306$; $W_{ipsi} = 91$; $p_{ipsi} = 0.0052$; $p_{corr,\ ipsi} = 0.0306$; P600: $W = 101$; $p = 0.0106$; $p_{corr} = 0.0314$; N = 29).

We found a statistically significant increase in the θ-ERS in the response to 75-ms vibratory stimuli during TI compared to no-TI baseline (Fig. 7A and B; $W = 67$; $p = 0.0013$; N = 29).

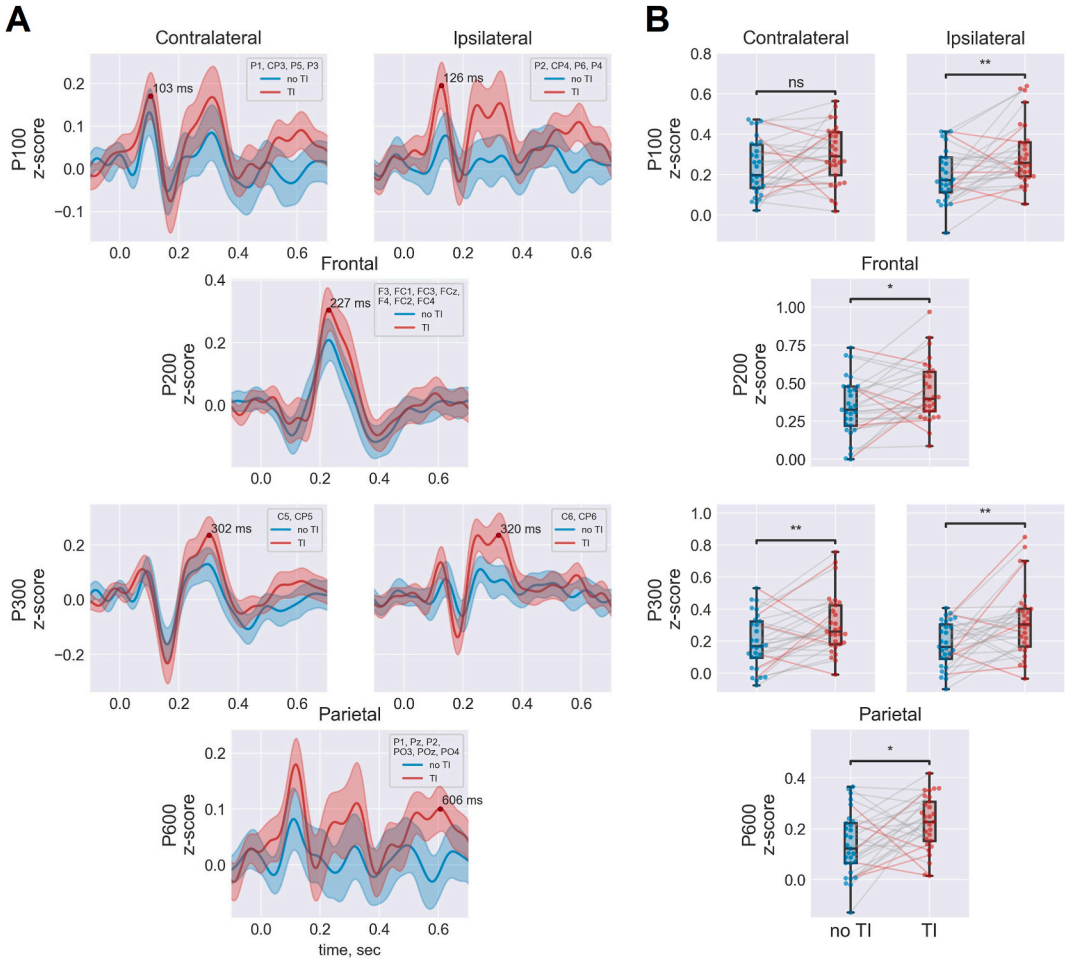

Fig. 6. A. Somatosensory event-related potentials to 75-ms vibrational pulses averaged across the target channels **B.** Boxplots of the mean amplitudes for the components in the contra- and ipsilateral hemispheres. In the boxplots, each point represents an individual participant, lines connect the measurements taken from the same participant, and red lines represent participants that were not able to voluntarily generate detectable μ-rhythm ERD. (For interpretation of the references to colour in this figure legend, the reader is referred to the Web version of this article.)

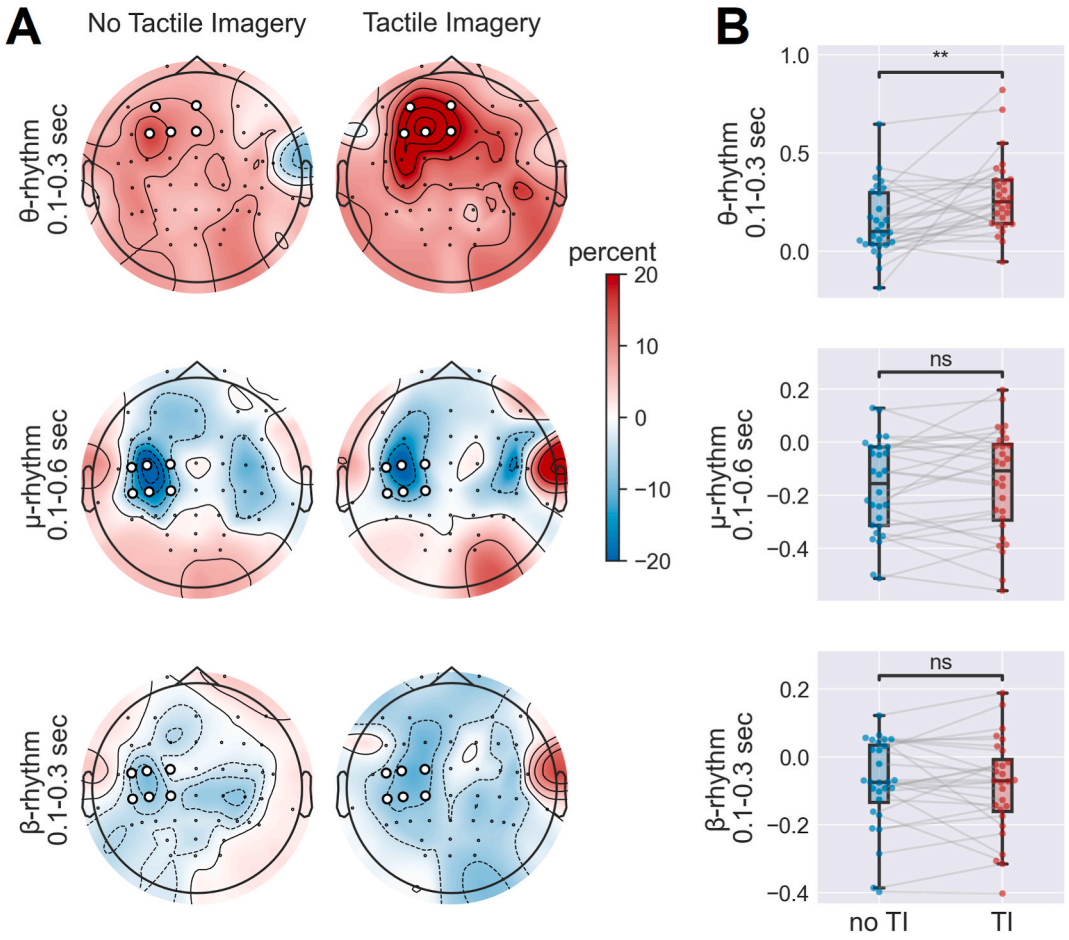

Fig. 7. **A.** Localization of the event-related time-frequency changes in response to 75-ms vibratory stimuli (target EEG channels are marked with white dots) **B.** Boxplots of the mean spectral power of the distinct event-related changes across the target channels.

We also found a strong correlation between the P200 amplitude during TI and θ-ERS during TI (Spearman's rank correlation, $r_S = 0.497$; $p = 0.007$; N = 29), and between P200 amplitude during TI and θ-ERS in no-TI baseline (Spearman's rank correlation, $r_S = 0.627$; $p = 0.0004$; N = 29). No statistically significant correlations between P200 amplitude and θ-ERS were found for the other combinations of conditions (Spearman's rank correlation; P200 at rest versus θ-ERS at rest: $r_S = 0.264$; $p = 0.17$; P200 at rest versus θ-ERS during TI: $r_S = 0.159$; $p = 0.418$; N = 29).

4. Discussion

In this study, we employed EEG recordings to examine cortical responses to TI. These EEG patterns were compared with the effects of continuous vibrostimulation applied to the fingertip. We found that vibrostimulation and TI modulated EEG oscillatory patterns in a similar way. Next, short vibrotactile pulses were utilized to probe sensorimotor modulations caused by TI. We found that TI indeed affected the responses to short vibratory pulses.

4.1. μ-rhythm ERD during tactile imagery practice

The analysis of the practice runs was of interest because those were the periods of learning where the inexperienced subjects attended the sensations evoked by vibrotactile stimulation and attempted to imagine them. During both the TS-practice and TI-practice, ERDs occurred in the μ-range (8–13 Hz). In the TI-practice trials, the ERD began 0.5 s following the visual cue that instructed imagery onset. The ERD persisted throughout the 8-s interval in both conditions (Fig. 2A and B). The μ-ERD was predominantly localized in the contralateral hemisphere with the strongest effects for the *C3-CP3* channels (Fig. 2B). These findings are generally consistent with the previous studies where TI was found to cause μ-rhythm ERD [18,25]. Thus, the μ-ERD appears to be a reliable indicator of an ongoing somatosensory processing of both real and imagined tactile stimuli.

Furthermore, an across-subject positive correlation was found between the ERD values during the TS- and TI-practice conditions

(see Fig. 3A), which strengthens the suggestion that imagined and real tactile stimuli are processed in a similar way and by the same cortical areas. The individual differences in the ERD values are most likely related to anatomical locations of the sensorimotor areas engaged and the specifics of the μ-rhythm in each participant. Indeed, in the motor imagery domain, SMR-based BCI performance varies depending on the individual brain structure [50,51]. Additionally, we found that subjects with a more prominent μ-rhythm peak exhibited greater ERD, which agrees with the Blankertz et al. [52] suggestion made for MI that the strength of the SMR-peak during the resting state could be used as a predictor of good BCI performance during imagery. Similarly, our results suggest that ERD-based decoding could be implemented in both TS and TI-based BCIs and perhaps ERD effects could be enhanced by BCI training. Overall, our present study aligns with the findings of Yao et al. [25,53], which demonstrated that BCI performance can be enhanced using tactile-induced ERD for calibration.

4.2. Tactile-imagery effects on SEPs

We found a significant increase in the ipsilateral P100 peak, with no changes observed in the contralateral P100. The ipsi-P100 had a delayed latency compared to the contra-P100, which suggests the involvement of transcallosal connectivity. We suggest that the P100 peak reflects the activation of the primary somatosensory cortex. This suggestion is supported by two observations: the contralateral predominance of the P100 and its relatively early timing, possibly corresponding to the P70 component reported in the studies using cutaneous electrical stimulation. A rather gradual onset of vibrotactile stimulation could explain the later peak latency compared to the response to electrical stimulation. The absence of the earlier components (P20 and P50) observed when electrical stimulation is used [54] could be also explained by the fact that the onset of vibrotactile stimulation was not abrupt enough.

The facilitation of P100 during TI could be explained by an attention-like mechanism where TI facilitates activity of the somatosensory cortex and makes it more responsive to peripheral inputs. Hämäläinen et al. [55] and Karhu & Tesche [39] showed that somatosensory spatial attention to the stimulated body part activated S2. Since both attention and mental imagery could affect sensory processing, separating the effects of attention and imagery could be challenging [21]. Therefore it is important to clarify the differences between attention and mental imagery. Attention is a mechanism of selection that enables focusing on the most important sensory inputs while discarding the other information, and imagery consists of formation, manipulation and transformation of mental images in the absence of physical stimulation [21,56,57]. Because of the similarity of brain processing involved in attention and imagery it was suggested that mental imagery is just a special form of attention [6,58]. Yet, studies of visual imagery showed that attention and mental imagery processes are driven by separate mechanisms [56,59].

While attention and imagery are distinct processes, they are closely linked. Indeed, performing a mental imagery task requires a shift in attention to the content of the imagery. Thus, visual imagery demands attentional shifts within a mental visuospatial representation [60] whereas a tactile imagery task involves directing attention within the peri-personal space and focusing on the site of imagined perception [24].

Subregions of S1 could have different roles in TI. Specifically, the BA3a subregion of S1 processes proprioceptive information from muscles and joints, and subregions BA3b, 1, and 2 process the signals from the skin [61]. BA2 is a higher-order hierarchical level that integrates both skin and proprioceptive signals. TS activates all S1 subregions in a somatotopic manner whereas TI preferentially engages BA2 via top-down pathways [17,30]. Consequently, the lack of a significant change in the contralateral P100 could be related to the fact that TI acts at a hierarchically higher BA2 subregion.

Activation of S2 in the present experiments is also likely because vibrotactile stimulation activates Pacinian afferents, which project strongly to S2 [62]. According to perceptual-grounding theory [24,40], the imagery of vibration-related tactile sensations should activate the corresponding S2 regions. In addition to the P100 peak, a later centrally localized positive SEP was observed in response to tactile stimulation with a latency of approximately 300 ms. The bilateral distribution and late latency of this peak suggests that it originated from S2 [38,55]. The significant increase in P300 in both hemispheres during TI is consistent with the role of S2 in the perceptual grounding of tactile images. Interestingly, the contralateral P300 had a shorter latency than the ipsilateral one, suggesting that ipsilateral activation could be mediated by transcallosal connections [38,39]. Yet, our data are insufficient for testing this hypothesis. The ipsilateral P300 could also originate from the subcortical structures (*e.g.* thalamus, given its connections with both S1 and S2 [63].

Previous studies of mental imagery (including tactile) have focused primarily on the primary sensory areas, which are thought to be principal contributors to mental imagery [64–66]. However, similar to our study, Yoo et al. [17] showed that S2 is involved in tactile imagery. In their study, TI-induced S2 activation was limited to the contralateral hemisphere and so we also expected the current study to show a contralateral predominance of the TI effects. Surprisingly, we found a greater increase in ipsilateral SEP peaks (P100 and P300). To explain the unexpected lateralization of TI effects on SEPs, we propose several hypotheses. First, the contralateral somatosensory areas could have been the most active one during TS because of the inputs generated by physical stimulation whereas the absence of these inputs during TI produced a weaker activity of the contralateral areas [67,68]. On the other hand, in response to TS at no-TI baseline condition, the ipsilateral regions were probably less activated [68], and TI caused facilitation that could have led to a stronger increase in the amplitude of the ipsi-SEPs. Second, ipsilateral SEPs were more likely to be elicited via transcallosal connections, with their peak amplitude depending on the excitability of both ipsilateral and contralateral cortical networks which in turn could participate in the interhemispheric transfer but not SEP formation [69,70]. Thus, an increase in ipsilateral SEPs amplitude could have been elicited by the additive effects of both contralateral and ipsilateral networks. Moreover, since S2 is responsible for the intermanual transfer of tactile image while tactile learning [71], ipsi-S2 activation in TI could be related to a transfer of an imagined sensation into the somatosensory representation of the opposite hand.

The P600 component is often associated with the processing of syntactic and semantic information, language comprehension,

memory, and attention [72]. Despite the majority of studies interpret P600 as related to language processing, P600 is also shown to be modulated in non-linguistic tasks, such as digit span Wechsler test on working memory [73] and hollow-mask illusion task [74]. On the other hand, there is evidence that P300 and P600 could be interrelated and share neural sources [75]. In line with this notion, we suggest that P600 facilitation in the TI condition could reflect the increased cognitive load and attentive focusing on the incoming stimuli caused by TI.

4.3. Frontal activation patterns modulated by tactile imagery and the role of working memory

We observed a θ-activity synchronization evoked by tactile stimuli that increased in the contralateral frontal area as TI continued. The frontal θ-increase is known to be associated with top-down memory processes [37]. Previous research suggested that the lateral prefrontal cortex (LFPC) is involved in tactile working memory [76,77]. Accordingly, we hypothesize that the observed θ-increase in the tactile imagery condition is an indicator of activation in the lateral prefrontal cortex (LPFC), which in turn could be caused by neural processing associated with TI. This hypothesis is supported by previous studies highlighting the role of the left inferior frontal gyrus, a part of the LPFC, in TI [24].

Consistent with these findings, the increased θ-ERS observed in our study likely signifies activation of the cortical network involved in the processing and integrating sensory information from working memory during mental image construction. However, it is worth noting that time-locked EEG deflections could be misleadingly interpreted as event-related synchronization (ERS) in the θ-range, potentially leading to misinterpretation of θ-ERS induced by external stimuli [78]. We found a frontal-localized P200 SEP peak, which could be mistakenly identified as θ-ERS on time-frequency graphs. Notably, θ-ERS showed a distinct localization in the contralateral frontal EEG channels, whereas the frontal P200 showed a broader distribution across frontal channels in both hemispheres (Figs. 4 and 7), and correlation analysis did not reveal any significant associations between θ-ERS and P200 peak amplitude in no-TI condition (Spearman's rank correlation; P200 no-TI versus θ-ERS no-TI: $r_S = 0.264$; $p = 0.17$; $N = 29$).

We observed a statistically significant increase in the P200 peak during TI (Fig. 4), which could have been related to LPFC activation during TI. The literature on mental imagery suggests that the LPFC is involved in the active construction of a mental image, regardless of the content being imagined [14,20,21,24,79]. At the same time, several studies have suggested that imagery can be conceptualized as an active dynamic that reactivates experienced sensations from memory [24,30,80]. This effect could also explain the observed increase in P300 during TI [81,82].

Our current results and the literature support the suggestion that incoming tactile information during TI is processed, among other areas, in the frontal cortex in order to store experienced sensations in memory (a bottom-up process) and retrieve for tactile imagery (a top-down process). This processing could be manifested as elevated frontal θ-oscillations and the P200 peak (Fig. 8). At the hierarchically lower level, tactile stimuli are processed in somatosensory cortices (S1, S2), which are interconnected. Here an interplay could take place between the top-down and bottom-up streams: the content of the mental imagery is unpacked from working memory thus initiating a perceptual grounding process, *i.e.* a reversal of perception that activates the somatosensory cortices where the descending signals result in an additive facilitation of these areas.

4.4. Tactile imagery for BCI-control and neurorehabilitation

As well as tactile imagery leading to prominent ERD [18], these modulations can be used for BCI-control based on sensorimotor EEG rhythms as an independent controlling source [25,83] and as a supplementary to the motor imagery-based BCI [84]. The usage of somatosensory-based BCI could be helpful for clinical rehabilitation of sensorimotor impairments (*e.g.* after strokes or neurotrauma) and phantom pain.

In the recent study we observed an enhanced cortical somatosensory processing associated with TI. TI could also induce brain plasticity [85,86]. The usage of SEP is suitable for BCI control [87,88], and in line with this suggestion, the TI approach could improve the performance of these BCI systems. The other important impact of our study is the usage of SEPs increase as a measurement method to assess TI performance.

4.5. Limitations

In the current study we showed that TI affects cortical responses to the application of short vibrotactile stimuli to the fingertip. The study has several limitations. Thus, a questionnaire could have been useful like the Vividness of Tactile Imagery Questionnaire (VTIQ) proposed by Nierhaus et al. [66]. Additionally, we did not collect data which could have clarified the correlation between electrophysiological measures and individual psychological characteristics. We suggested that some of the effects could be related to memory and attentional processes involved in the mental imagery task. Further experimental work should clarify these mechanisms. In addition, conventional EEG recordings do not provide precise information on the localization of cortical SEP sources because of the insufficient spatial resolution. Finally, the vibrostimulation method we used in this study has some disadvantages, including limitations in precisely controlling the stimuli. Such stimulation affects not only cutaneous receptors but also proprioceptive (kinesthetic) receptors, which are part of muscle sensation and could contribute to motor-related effects. In order to properly distinguish the effects of TI from the motor-related effects, somatosensory stimuli will have to be used which selectively activate pressure and temperature receptors of the skin.

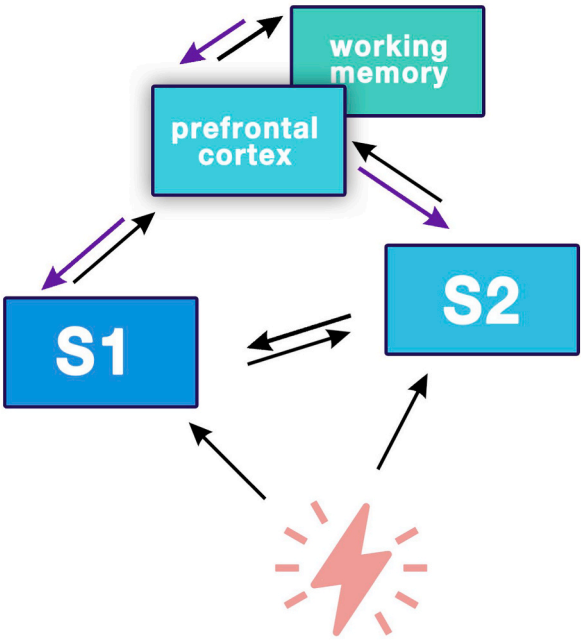

Fig. 8. Schematic representation of the effects of the imagery process on the processing of real tactile stimuli, which we propose on the basis of the results obtained. Black arrows represent normal somatosensory processing. Blue arrows represent facilitation of processing during tactile imagery. (For interpretation of the references to colour in this figure legend, the reader is referred to the Web version of this article.)

5. Conclusion

In this study, participants engaged in a TI task during which contralateral μ-rhythm ERD was positively correlated, across the participants, with the ERD observed during actual vibrostimulation. TI induces alterations in several SEP components localized across sensorimotor and frontal cortices. The observed differences suggest that TI facilitates cortical processing, particularly in the somatosensory cortex (as evident from the changes in the P100 and P300 components) and frontal areas which direct somatosensory attention and maintain working memory. Our observations align with previous neurovisualization studies on TI and contribute additional data to the existing body of knowledge. The SEP components identified in our study could serve as a methodology for noninvasively assessing cortical mechanisms of mental imagery.

CRediT authorship contribution statement

Marina Morozova: Writing – review & editing, Writing – original draft, Visualization, Methodology, Investigation, Formal analysis, Data curation, Conceptualization. **Lev Yakovlev:** Writing – review & editing, Writing – original draft, Supervision, Project administration. **Nikolay Syrov:** Writing – review & editing, Writing – original draft, Visualization, Supervision, Project administration. **Mikhail Lebedev:** Writing – review & editing, Supervision, Resources, Project administration, Funding acquisition. **Alexander Kaplan:** Writing – review & editing, Supervision, Resources, Project administration.

Data availability

The dataset collected and analyzed during the current study is available from the corresponding author on reasonable request.

Declaration of competing interest

The authors declare that they have no known competing financial interests or personal relationships that could have appeared to influence the work reported in this paper.

Acknowledgments

This work is supported by the Russian Science Foundation under grant #21-75-30024.

References

[1] M.J. Farah, The neural basis of mental imagery, Trends Neurosci. 12 (1989) 395–399, https://doi.org/10.1016/0166-2236(89)90079-9.
[2] B. Nanay, Multimodal mental imagery, Cortex 105 (2018) 125–134, https://doi.org/10.1016/j.cortex.2017.07.006.
[3] J. Decety, The neurophysiological basis of motor imagery, Behav. Brain Res. 77 (1996) 45–52, https://doi.org/10.1016/0166-4328(95)00225-1.
[4] D.J. Crammond, Motor imagery: never in your wildest dream, Trends Neurosci. 20 (1997) 54–57, https://doi.org/10.1016/s0166-2236(96)30019-2.
[5] M. Jeannerod, V. Frak, Mental imaging of motor activity in humans, Curr. Opin. Neurobiol. 9 (1999) 735–739, https://doi.org/10.1016/s0959-4388(99)00038-0.
[6] Z.W. Pylyshyn, Mental imagery: in search of a theory, Behav. Brain Sci. 25 (2002) 157–182, https://doi.org/10.1017/s0140525x02000043. ; discussion 182-237.
[7] L. Warner, M.E. McNeill, Mental imagery and its potential for physical therapy, Phys. Ther. 68 (1988) 516–521, https://doi.org/10.1093/ptj/68.4.516.
[8] R. Van Leeuwen, T.J. Inglis, Mental practice and imagery: a potential role in stroke rehabilitation, Phys. Ther. Rev. 3 (1998) 47–52, https://doi.org/10.1179/ptr.1998.3.1.47.
[9] A. Zimmermann-Schlatter, C. Schuster, M.A. Puhan, E. Siekierka, J. Steurer, Efficacy of motor imagery in post-stroke rehabilitation: a systematic review, J. Neuroengineering Rehabil. 5 (2008) 8, https://doi.org/10.1186/1743-0003-5-8.
[10] S. Di Nuovo, V. De La Cruz, D. Conti, S. Buono, A. Di Nuovo, Mental imagery: rehabilitation through simulation, Life Span Disabil 17 (2014) 89–118.
[11] J. Pearson, T. Naselaris, E.A. Holmes, S.M. Kosslyn, Mental imagery: functional mechanisms and clinical applications, Trends Cogn. Sci. 19 (2015) 590–602, https://doi.org/10.1016/j.tics.2015.08.003.
[12] S.M. Kosslyn, W.L. Thompson, When is early visual cortex activated during visual mental imagery? Psychol. Bull. 129 (2003) 723–746, https://doi.org/10.1037/0033-2909.129.5.723.
[13] L. Nyberg, R. Habib, A.R. McIntosh, E. Tulving, Reactivation of encoding-related brain activity during memory retrieval, Proc. Natl. Acad. Sci. U. S. A. 97 (2000) 11120–11124, https://doi.org/10.1073/pnas.97.20.11120.
[14] S.S. Yoo, C.U. Lee, B.G. Choi, Human brain mapping of auditory imagery: event-related functional MRI study, Neuroreport 12 (2001) 3045–3049, https://doi.org/10.1097/00001756-200110080-00013.
[15] J. Djordjevic, R.J. Zatorre, M. Petrides, J.A. Boyle, M. Jones-Gotman, Functional neuroimaging of odor imagery, Neuroimage 24 (2005) 791–801, https://doi.org/10.1016/j.neuroimage.2004.09.035.
[16] J. Plailly, C. Delon-Martin, J.-P. Royet, Experience induces functional reorganization in brain regions involved in odor imagery in perfumers, Hum. Brain Mapp. 33 (2012) 224–234, https://doi.org/10.1002/hbm.21207.
[17] S.-S. Yoo, D.K. Freeman, J.J. McCarthy, F.A. Jolesz, Neural substrates of tactile imagery: a functional MRI study, Neuroreport 14 (2003) 581–585, https://doi.org/10.1097/00001756-200303240-00011.
[18] L. Yakovlev, N. Syrov, A. Miroshnikov, M. Lebedev, A. Kaplan, Event-related desynchronization induced by tactile imagery: an EEG study, eNeuro (2023), https://doi.org/10.1523/ENEURO.0455-22.2023.
[19] S.M. Kosslyn, G. Ganis, W.L. Thompson, Neural foundations of imagery, Nat. Rev. Neurosci. 2 (2001) 635–642, https://doi.org/10.1038/35090055.
[20] C. McNorgan, A meta-analytic review of multisensory imagery identifies the neural correlates of modality-specific and modality-general imagery, Front. Hum. Neurosci. 6 (2012) 285, https://doi.org/10.3389/fnhum.2012.00285.
[21] J. Pearson, The human imagination: the cognitive neuroscience of visual mental imagery, Nat. Rev. Neurosci. 20 (2019) 624–634, https://doi.org/10.1038/s41583-019-0202-9.
[22] M. Lotze, U. Halsband, Motor imagery, J. Physiol. Paris 99 (2006) 386–395, https://doi.org/10.1016/j.jphysparis.2006.03.012.
[23] A.M. Ladda, F. Lebon, M. Lotze, Using motor imagery practice for improving motor performance—a review, Brain Cogn 150 (2021), https://doi.org/10.1016/j.bandc.2021.105705.
[24] T.T. Schmidt, D. Ostwald, F. Blankenburg, Imaging tactile imagery: changes in brain connectivity support perceptual grounding of mental images in primary sensory cortices, Neuroimage 98 (2014) 216–224, https://doi.org/10.1016/j.neuroimage.2014.05.014.
[25] L. Yao, N. Jiang, N. Mrachacz-Kersting, X. Zhu, D. Farina, Y. Wang, Performance variation of a somatosensory BCI based on imagined sensation: a large population study, IEEE Trans. Neural Syst. Rehabil. Eng. Publ. IEEE Eng. Med. Biol. Soc. 30 (2022) 2486–2493, https://doi.org/10.1109/TNSRE.2022.3198970.
[26] A. Miroshnikov, L. Yakovlev, N. Syrov, A. Vasilyev, A. Berkmush-Antipova, F. Golovanov, A. Kaplan, Differential hemodynamic responses to motor and tactile imagery: insights from multichannel fNIRS mapping, Brain Topogr. 38 (2024) 4, https://doi.org/10.1007/s10548-024-01075-x.
[27] P. Sengupta, K. Lakshminarayanan, Cortical activation and BCI performance during brief tactile imagery: a comparative study with motor imagery, Behav. Brain Res. 459 (2024) 114760, https://doi.org/10.1016/j.bbr.2023.114760.
[28] P. Arpaia, A. Esposito, A. Natalizio, M. Parvis, How to successfully classify EEG in motor imagery BCI: a metrological analysis of the state of the art, J. Neural. Eng. 19 (2022), https://doi.org/10.1088/1741-2552/ac74e0.
[29] A.W. de Borst, B. de Gelder, fMRI-based multivariate pattern analyses reveal imagery modality and imagery content specific representations in primary somatosensory, motor and auditory cortices, Cereb. Cortex N. Y. N 1991 27 (2017) 3994–4009, https://doi.org/10.1093/cercor/bhw211.
[30] T.T. Schmidt, F. Blankenburg, The somatotopy of mental tactile imagery, Front. Hum. Neurosci. 13 (2019), https://doi.org/10.3389/fnhum.2019.00010.
[31] L. Bashford, I. Rosenthal, S. Kellis, K. Pejsa, D. Kramer, B. Lee, C. Liu, R.A. Andersen, The neurophysiological representation of imagined somatosensory percepts in human cortex, J. Neurosci. Off. J. Soc. Neurosci. 41 (2021) 2177–2185, https://doi.org/10.1523/JNEUROSCI.2460-20.2021.
[32] G. Pfurtscheller, C. Neuper, Motor imagery activates primary sensorimotor area in humans, Neurosci. Lett. 239 (1997) 65–68, https://doi.org/10.1016/s0304-3940(97)00889-6.
[33] C. Neuper, M. Wörtz, G. Pfurtscheller, ERD/ERS patterns reflecting sensorimotor activation and deactivation, Prog. Brain Res. 159 (2006) 211–222, https://doi.org/10.1016/S0079-6123(06)59014-4.
[34] T.W. Boonstra, A. Daffertshofer, M. Breakspear, P.J. Beek, Multivariate time-frequency analysis of electromagnetic brain activity during bimanual motor learning, Neuroimage 36 (2007) 370–377, https://doi.org/10.1016/j.neuroimage.2007.03.012.
[35] F. Freyer, R. Becker, H.R. Dinse, P. Ritter, State-dependent perceptual learning, J. Neurosci. 33 (2013) 2900–2907, https://doi.org/10.1523/JNEUROSCI.4039-12.2013.
[36] J.A. Pineda, The functional significance of mu rhythms: translating “seeing” and “hearing” into “doing,”, Brain Res. Brain Res. Rev. 50 (2005) 57–68, https://doi.org/10.1016/j.brainresrev.2005.04.005.
[37] W. Klimesch, P. Sauseng, S. Hanslmayr, EEG alpha oscillations: the inhibition-timing hypothesis, Brain Res. Rev. 53 (2007) 63–88, https://doi.org/10.1016/j.brainresrev.2006.06.003.
[38] K. Hoechstetter, A. Rupp, A. Stancák, H.M. Meinck, C. Stippich, P. Berg, M. Scherg, Interaction of tactile input in the human primary and secondary somatosensory cortex–a magnetoencephalographic study, Neuroimage 14 (2001) 759–767, https://doi.org/10.1006/nimg.2001.0855.
[39] J. Karhu, C.D. Tesche, Simultaneous early processing of sensory input in human primary (SI) and secondary (SII) somatosensory cortices, J. Neurophysiol. 81 (1999) 2017–2025, https://doi.org/10.1152/jn.1999.81.5.2017.
[40] L.W. Barsalou, Grounded cognition, Annu. Rev. Psychol. 59 (2008) 617–645, https://doi.org/10.1146/annurev.psych.59.103006.093639.
[41] M. Takemi, Y. Masakado, M. Liu, J. Ushiba, Event-related desynchronization reflects downregulation of intracortical inhibition in human primary motor cortex, J. Neurophysiol. 110 (2013) 1158–1166, https://doi.org/10.1152/jn.01092.2012.
[42] K. Aono, S. Miyashita, Y. Fujiwara, M. Kodama, K. Hanayama, Y. Masakado, J. Ushiba, Relationship between event-related desynchronization and cortical excitability in healthy subjects and stroke patients, Tokai J. Exp. Clin. Med. 38 (2013) 123–128.
[43] A. Vasilyev, S. Liburkina, L. Yakovlev, O. Perepelkina, A. Kaplan, Assessing motor imagery in brain-computer interface training: psychological and neurophysiological correlates, Neuropsychologia 97 (2017) 56–65, https://doi.org/10.1016/j.neuropsychologia.2017.02.005.

[44] P.M. Cowley, B.C. Clark, L.L. Ploutz-Snyder, Kinesthetic motor imagery and spinal excitability: the effect of contraction intensity and spatial localization, Clin. Neurophysiol. Off. J. Int. Fed. Clin. Neurophysiol. 119 (2008) 1849–1856, https://doi.org/10.1016/j.clinph.2008.04.004.

[45] M. Takemi, Y. Masakado, M. Liu, J. Ushiba, Sensorimotor event-related desynchronization represents the excitability of human spinal motoneurons, Neuroscience 297 (2015) 58–67, https://doi.org/10.1016/j.neuroscience.2015.03.045.

[46] A.N. Vasilyev, Y.O. Nuzhdin, A.Y. Kaplan, Does real-time feedback affect sensorimotor EEG patterns in routine motor imagery practice? Brain Sci. 11 (2021) 1234, https://doi.org/10.3390/brainsci11091234.

[47] N. Bigdely-Shamlo, T. Mullen, C. Kothe, K.-M. Su, K.A. Robbins, The PREP pipeline: standardized preprocessing for large-scale EEG analysis, Front. Neuroinformatics 9 (2015), https://doi.org/10.3389/fninf.2015.00016.

[48] E. Maris, R. Oostenveld, Nonparametric statistical testing of EEG- and MEG-data, J. Neurosci. Methods 164 (2007) 177–190, https://doi.org/10.1016/j.jneumeth.2007.03.024.

[49] J. Sassenhagen, D. Draschkow, Cluster-based permutation tests of MEG/EEG data do not establish significance of effect latency or location, Psychophysiology 56 (2019) e13335, https://doi.org/10.1111/psyp.13335.

[50] S. Halder, B. Varkuti, M. Bogdan, A. Kübler, W. Rosenstiel, R. Sitaram, N. Birbaumer, Prediction of brain-computer interface aptitude from individual brain structure, Front. Hum. Neurosci. 7 (2013), https://doi.org/10.3389/fnhum.2013.00105.

[51] K. Kasahara, C.S. DaSalla, M. Honda, T. Hanakawa, Neuroanatomical correlates of brain-computer interface performance, Neuroimage 110 (2015) 95–100, https://doi.org/10.1016/j.neuroimage.2015.01.055.

[52] B. Blankertz, C. Sannelli, S. Halder, E.M. Hammer, A. Kübler, K.-R. Müller, G. Curio, T. Dickhaus, Neurophysiological predictor of SMR-based BCI performance, Neuroimage 51 (2010) 1303–1309, https://doi.org/10.1016/j.neuroimage.2010.03.022.

[53] L. Yao, X. Sheng, N. Mrachacz-Kersting, X. Zhu, D. Farina, N. Jiang, Sensory stimulation training for BCI system based on somatosensory attentional orientation, IEEE Trans. Biomed. Eng. 66 (2019) 640–646, https://doi.org/10.1109/TBME.2018.2852755.

[54] M. Novičić, A.M. Savić, Somatosensory event-related potential as an electrophysiological correlate of endogenous spatial tactile attention: prospects for electrotactile brain-computer interface for sensory training, Brain Sci. 13 (2023) 766, https://doi.org/10.3390/brainsci13050766.

[55] H. Hämäläinen, J. Kekoni, M. Sams, K. Reinikainen, R. Näätänen, Human somatosensory evoked potentials to mechanical pulses and vibration: contributions of SI and SII somatosensory cortices to P50 and P100 components, Electroencephalogr. Clin. Neurophysiol. 75 (1990) 13–21, https://doi.org/10.1016/0013-4694(90)90148-D.

[56] W.L. Thompson, Y. Hsiao, S.M. Kosslyn, Dissociation between visual attention and visual mental imagery, J. Cogn. Psychol. 23 (2011) 256–263, https://doi.org/10.1080/20445911.2011.477810.

[57] B. Bazgir, A. Shamseddini, J.A. Hogg, F. Ghadiri, M. Bahmani, J.A. Diekfuss, Is cognitive control of perception and action via attentional focus moderated by motor imagery? BMC Psychol 11 (2023) 12, https://doi.org/10.1186/s40359-023-01047-z.

[58] J.R. Pani, Mental imagery is simultaneously symbolic and analog, Behav. Brain Sci. 25 (2002) 205–206, https://doi.org/10.1017/s0140525x02450042.

[59] J. Pearson, C.W.G. Clifford, F. Tong, The functional impact of mental imagery on conscious perception, Curr. Biol. 18 (2008) 982–986, https://doi.org/10.1016/j.cub.2008.05.048.

[60] S. Kosslyn, Mental images and the brain, Cogn. Neuropsychol. 22 (2005) 333–347, https://doi.org/10.1080/02643290442000130.

[61] R. Martuzzi, W. van der Zwaag, J. Farthouat, R. Gruetter, O. Blanke, Human finger somatotopy in areas 3b, 1, and 2: a 7T fMRI study using a natural stimulus, Hum. Brain Mapp. 35 (2014) 213–226, https://doi.org/10.1002/hbm.22172.

[62] G.R. Fisher, B. Freeman, M.J. Rowe, Organization of parallel projections from Pacinian afferent fibers to somatosensory cortical areas I and II in the cat, J. Neurophysiol. 49 (1983) 75–97, https://doi.org/10.1152/jn.1983.49.1.75.

[63] Y. Song, Q. Su, Q. Yang, R. Zhao, G. Yin, W. Qin, G.D. Iannetti, C. Yu, M. Liang, Feedforward and feedback pathways of nociceptive and tactile processing in human somatosensory system: a study of dynamic causal modeling of fMRI data, Neuroimage 234 (2021) 117957, https://doi.org/10.1016/j.neuroimage.2021.117957.

[64] R. Sparing, F.M. Mottaghy, G. Ganis, W.L. Thompson, R. Töpper, S.M. Kosslyn, A. Pascual-Leone, Visual cortex excitability increases during visual mental imagery–a TMS study in healthy human subjects, Brain Res. 938 (2002) 92–97, https://doi.org/10.1016/s0006-8993(02)02478-2.

[65] A. Kaas, R. Goebel, G. Valente, B. Sorger, Topographic somatosensory imagery for real-time fMRI brain-computer interfacing, Front. Hum. Neurosci. 13 (2019) 427, https://doi.org/10.3389/fnhum.2019.00427.

[66] T. Nierhaus, S. Wesolek, D. Pach, C.M. Witt, F. Blankenburg, T.T. Schmidt, Content representation of tactile mental imagery in primary somatosensory cortex, eNeuro 10 (2023), https://doi.org/10.1523/ENEURO.0408-22.2023. ENEURO.0408-0422.2023.

[67] M.T. Carrillo-de-la-Peña, S. Galdo-Alvarez, C. Lastra-Barreira, Equivalent is not equal: primary motor cortex (MI) activation during motor imagery and execution of sequential movements, Brain Res. 1226 (2008) 134–143, https://doi.org/10.1016/j.brainres.2008.05.089.

[68] G. Lamp, P. Goodin, S. Palmer, E. Low, A. Barutchu, L.M. Carey, Activation of bilateral secondary somatosensory cortex with right hand touch stimulation: a meta-analysis of functional neuroimaging studies, Front. Neurol. 9 (2018) 1129, https://doi.org/10.3389/fneur.2018.01129.

[69] T. Hansson, T. Brismar, Tactile stimulation of the hand causes bilateral cortical activation: a functional magnetic resonance study in humans, Neurosci. Lett. 271 (1999) 29–32, https://doi.org/10.1016/s0304-3940(99)00508-x.

[70] P. Ragert, T. Nierhaus, L.G. Cohen, A. Villringer, Interhemispheric interactions between the human primary somatosensory cortices, PLoS One 6 (2011) e16150, https://doi.org/10.1371/journal.pone.0016150.

[71] R.M. Ridley, G. Ettlinger, Impaired tactile learning and retention after removals of the second somatic sensory projection cortex (SII) in the monkey, Brain Res. 109 (1976) 656–660, https://doi.org/10.1016/0006-8993(76)90048-2.

[72] I. Bornkessel-Schlesewsky, M. Schlesewsky, An alternative perspective on “semantic P600” effects in language comprehension, Brain Res. Rev. 59 (2008) 55–73, https://doi.org/10.1016/j.brainresrev.2008.05.003.

[73] I. Kalatzis, N. Piliouras, D. Glotsos, E. Ventouras, C. Papageorgiou, A. Rabavilas, C. Soldatos, D. Cavouras, Identifying differences in the P600 component of ERP-signals between OCD patients and controls employing a PNN-based majority vote classification scheme, Conf. Proc. Annu. Int. Conf. IEEE Eng. Med. Biol. Soc. IEEE Eng. Med. Biol. Soc. Annu. Conf. 2005 (2005) 3994–3997, https://doi.org/10.1109/IEMBS.2005.1615337.

[74] D. Dima, W. Dillo, C. Bonnemann, H.M. Emrich, D.E. Dietrich, Reduced P300 and P600 amplitude in the hollow-mask illusion in patients with schizophrenia, Psychiatry Res 191 (2011) 145–151, https://doi.org/10.1016/j.pscychresns.2010.09.015.

[75] J. Sassenhagen, C.J. Fiebach, Finding the P3 in the P600: decoding shared neural mechanisms of responses to syntactic violations and oddball targets, Neuroimage 200 (2019) 425–436, https://doi.org/10.1016/j.neuroimage.2019.06.048.

[76] R. Auksztulewicz, B. Spitzer, D. Goltz, F. Blankenburg, Impairing somatosensory working memory using rTMS, Eur. J. Neurosci. 34 (2011) 839–844, https://doi.org/10.1111/j.1460-9568.2011.07797.x.

[77] B. Spitzer, D. Goltz, E. Wacker, R. Auksztulewicz, F. Blankenburg, Maintenance and manipulation of somatosensory information in ventrolateral prefrontal cortex, Hum. Brain Mapp. 35 (2013) 2412–2423, https://doi.org/10.1002/hbm.22337.

[78] J. Harper, S.M. Malone, E.M. Bernat, Theta and delta band activity explain N2 and P3 ERP component activity in a go/no-go task, Clin. Neurophysiol. Off. J. Int. Fed. Clin. Neurophysiol. 125 (2014) 124–132, https://doi.org/10.1016/j.clinph.2013.06.025.

[79] A. Ishai, L.G. Ungerleider, J.V. Haxby, Distributed neural systems for the generation of visual images, Neuron 28 (2000) 979–990, https://doi.org/10.1016/s0896-6273(00)00168-9.

[80] J. Theeuwes, A.F. Kramer, D.E. Irwin, Attention on our mind: the role of spatial attention in visual working memory, Acta Psychol. 137 (2011) 248–251, https://doi.org/10.1016/j.actpsy.2010.06.011.

[81] T. Kida, Y. Nishihira, A. Hatta, T. Wasaka, Somatosensory N250 and P300 during discrimination tasks, Int. J. Psychophysiol. 48 (2003) 275–283, https://doi.org/10.1016/S0167-8760(03)00021-7.

[82] J. Polich, Updating P300: an integrative theory of P3a and P3b, Clin. Neurophysiol. Off. J. Int. Fed. Clin. Neurophysiol. 118 (2007) 2128–2148, https://doi.org/10.1016/j.clinph.2007.04.019.

[83] L. Yao, N. Mrachacz-Kersting, X. Sheng, X. Zhu, D. Farina, N. Jiang, A multi-class BCI based on somatosensory imagery, IEEE Trans. Neural Syst. Rehabil. Eng. 26 (2018) 1508–1515, https://doi.org/10.1109/TNSRE.2018.2848883.
[84] L. Yao, X. Sheng, D. Zhang, N. Jiang, D. Farina, X. Zhu, A BCI system based on somatosensory attentional orientation, IEEE Trans. Neural Syst. Rehabil. Eng. 25 (2017) 81–90, https://doi.org/10.1109/TNSRE.2016.2572226.
[85] Y. Bunno, Imagery strategy affects spinal motor neuron excitability: using kinesthetic and somatosensory imagery, Neuroreport 30 (2019) 463–467, https://doi.org/10.1097/WNR.0000000000001218.
[86] M. Morozova, A. Nasibullina, L. Yakovlev, N. Syrov, A. Kaplan, M. Lebedev, Tactile versus motor imagery: differences in corticospinal excitability assessed with single-pulse TMS, *Scientific Reports 14* (1) (2024) 14862, https://doi.org/10.1038/s41598-024-64665-6.
[87] C. Chu, J. Luo, X. Tian, X. Han, S. Guo, A P300 brain-computer interface paradigm based on electric and vibration simple command tactile stimulation, Front. Hum. Neurosci. 15 (2021), https://doi.org/10.3389/fnhum.2021.641357.
[88] A.M. Savić, M. Novičić, O. Đorđević, L. Konstantinović, V. Miler-Jerković, Novel electrotactile brain-computer interface with somatosensory event-related potential based control, Front. Hum. Neurosci. 17 (2023) 1096814, https://doi.org/10.3389/fnhum.2023.1096814.